

COMPUTATIONAL DESIGN OF Mn_4 MOLECULES WITH STRONG INTRAMOLECULAR EXCHANGE COUPLING

NGUYEN ANH TUAN, NGUYEN VAN THANH,
TRAN THI THUY NU, AND NGUYEN HUY SINH

Faculty of Physics, Hanoi University of Science

VU VAN KHAI

Faculty of Physics, Hanoi University of Science

and

National University of Civil Engineering

DAM HIEU CHI

Faculty of Physics, Hanoi University of Science

and

School of Materials Science,

Japan Advanced Institute of Science and Technology,

1-1, Asahidai, Nomi, Ishikawa, 923-1292 Japan

SHIN-ICHI KATAYAMA

School of Materials Science,

Japan Advanced Institute of Science and Technology,

1-1, Asahidai, Nomi, Ishikawa, 923-1292 Japan

Abstract. *The geometric and electronic structures of $[Mn^{4+}Mn_3^{3+}(\mu_3-L^{2-})_3(\mu_3-X^-)(OAc)_3(dbm)_3]$ ($L = O, X = F, dbmH =$ dibenzoyl-methane) molecule has been studied by first-principles calculations. It was shown in our previous paper that the ferrimagnetic structure of $Mn^{4+}Mn_3^{3+}$ molecules is determined by the π type hybridization between the d_{z^2} orbitals at the three high-spin Mn^{3+} ions and the t_{2g} orbitals at the Mn^{4+} ion by the p orbitals at the μ_3-L^{2-} ions. To design new $Mn^{4+}Mn_3^{3+}$ molecules having much more stable ferrimagnetic state, one approach is suggested. That is controlling the $Mn^{4+}-(\mu_3-L^{2-})-Mn^{3+}$ exchange pathways by rational variation in μ_3-L ligands to strengthen the hybridization between Mn ions. By this ligand variation, J_{AB} can be enhanced by a factor of 3. Our results should facilitate the rational synthesis of new single-molecule magnets.*

I. INTRODUCTION

Single-molecule magnets (SMMs) are molecules that can function as magnets below their blocking temperature (T_B) are being extensively studied due to their potential technological applications to molecular spintronics [1]. This behavior results from a high ground-state spin (S_T) combined with a large and negative Ising type of magnetoanisotropy, as measured by the axial zero-field splitting parameter (D). SMM consists of magnetic atoms connected and surrounded by ligands. The challenge of SMMs consists

in tailoring magnetic properties by specific modifications of the molecular units. The S_T results from local spin moments at magnetic ions (S_i) and exchange coupling between them (J_{ij}). Moreover, J_{ij} has to be important to well separate the ground spin state from the excited states [2–4]. Therefore, seeking possibilities of the enhancement of J_{ij} will be a way to develop SMMs.

In the framework of computational materials design, distorted cubane $[\text{Mn}^{4+}\text{Mn}_3^{3+}(\mu_3\text{-L}^{2-})_3(\mu_3\text{-X}^-)(\text{OAc})_3(\text{dbm})_3]$ ($\text{L} = \text{O}$; $\text{X} =$ an anionic ligand such as F, Cl, and Br; dbmH = dibenzoyl-methane) (hereafter $\text{Mn}^{4+}\text{Mn}_3^{3+}$) molecules [5,6] is one of the most attractive SMM systems because their interesting geometric structure and important magnetic quantities can be well estimated by first-principles calculations [7-10]. In our previous paper [7], by using first-principles calculations within generalized gradient approximation, the basic mechanism of the antiferromagnetic (AFM) interaction between the Mn^{4+} ion and the three high-spin Mn^{3+} ions in $\text{Mn}^{4+}\text{Mn}_3^{3+}$ molecules was analyzed. The AFM $\text{Mn}^{4+}\text{-Mn}^{3+}$ coupling (J_{AB}) is determined by the π type hybridization among the d_{z^2} orbitals at the Mn^{3+} sites and the t_{2g} orbitals at the Mn^{4+} site through the p orbitals at the $\mu_3\text{-L}^{2-}$ ions. This result allows us to predict that ferrimagnetic structure of $\text{Mn}^{4+}\text{Mn}_3^{3+}$ molecules will be the most stable with the $\text{Mn}^{4+}\text{-(}\mu_3\text{-L}^{2-}\text{)-Mn}^{3+}$ angle $\alpha \approx 90^\circ$, while synthesized $\text{Mn}^{4+}\text{Mn}_3^{3+}$ molecules have $\alpha \approx 95^\circ$. To design new $\text{Mn}^{4+}\text{Mn}_3^{3+}$ SMMs having much more stable ferrimagnetic state, one approach is suggested. That is controlling the $\text{Mn}^{4+}\text{-(}\mu_3\text{-L}^{2-}\text{)-Mn}^{3+}$ exchange pathways by rational variation in $\mu_3\text{-L}$ ligands to strengthen the hybridization between Mn ions. Our calculated results show that J_{AB} can be enhanced by a factor of 3 by using N-based ligands to form the exchange pathways between the Mn^{4+} and Mn^{3+} ions. Our results should facilitate the rational synthesis of new SMMs.

II. COMPUTATIONAL METHOD

To compute the geometric structure, electronic structure and effective exchange coupling parameters of Mn_4 molecules, the same reliable computational method as in our previous paper [7] is adopted. In this method, all calculations have been performed by using DMol³ code with the double numerical basis sets plus polarization functional (DNP) [11]. For the exchange correlation terms, the generalized gradient approximation (GGA) RPBE functional was used [12]. All-electron relativistic was used to describe the interaction between the core and valence electrons [13]. The real-space global cutoff radius was set to be 4.7 Å for all atoms. The spin-unrestricted DFT was used to obtain all results presented in this study. The atomic charge and magnetic moment were obtained by using the Mulliken population analysis [14]. The charge density is converged to 1×10^{-6} a.u. in the self-consistent calculation. In the optimization process, the energy, energy gradient, and atomic displacement are converged to 1×10^{-5} , 1×10^{-4} and 1×10^{-3} a.u., respectively. The total energy difference method was adopted to calculate the exchange coupling parameters of Mn_4 molecules [7]. To determine exactly the magnetic ground state of $\text{Mn}^{4+}\text{Mn}_3^{3+}$ molecules, all possible spin configurations of $\text{Mn}^{4+}\text{Mn}_3^{3+}$ molecules are probed, which are imposed as an initial condition of the structural optimization procedure. The number of spin configurations should be considered depending on the charge state of

manganese ions. In terms of the octahedral field, Mn⁴⁺ ions could, in principle, have only the high-spin state with configuration $d^3(t_{2g}^3, e_g^0)$, in which three d electrons occupy three different t_{2g} orbitals. The possible spin states of Mn³⁺ ion are the high-spin (HS) state with configuration $d^4(t_{2g}^3, e_g^1)$ and the low-spin (LS) state with configuration $d^4(t_{2g}^4, e_g^0)$. Additionally, the magnetic coupling between the Mn⁴⁺ ion at the A site and Mn³⁺ ions at the B site can be ferromagnetic (FM) or antiferromagnetic (AFM). Therefore, there are four spin configurations which should be considered for each Mn⁴⁺Mn₃³⁺ molecule, including: (i) AFM-HS, (ii) AFM-LS, (iii) FM-HS, and (iv) FM-LS.

III. RESULTS AND DISCUSSION

The geometric structures of synthesized distorted cubane [Mn⁴⁺Mn₃³⁺(μ_3 -L²⁻)₃(μ_3 -X⁻)(OAc)₃(dbm)₃]⁻ (L = O; X = an anionic ligand such as F, Cl, and Br; dbmH = dibenzoyl-methane) molecules [5,6] are depicted in Fig. 1. Previous experimental studies reported that each Mn⁴⁺Mn₃³⁺ molecule has C_{3v} symmetry, with the C_3 axis passing through Mn⁴⁺ and X⁻ ions. The [Mn₄(μ_3 -O)₃(μ_3 -X)] core can be simply viewed as a “distorted cubane”, in which the four Mn atoms are located at the corners of a trigonal pyramid, with a μ_3 -O²⁻ ion bridging each of the vertical faces and a μ_3 -X⁻ ion bridging the basal face. Three carboxylate (OAc) groups, forming three bridges between the A site (Mn⁴⁺ ion) and the B sites (Mn³⁺ ions), play an important role in stabilizing the distorted cubane geometry of the Mn₄O₃X core. Each peripheral-ligands dbm forms two coordinate bonds to complete the distorted octahedral geometry at each B site.

III.1. Modelling Mn₄ molecules

In this study, new distorted cubane Mn⁴⁺Mn₃³⁺ molecules have been designed by rational variations in the μ_3 -O, μ_3 -F, and dbm groups of the synthesized distorted cubane Mn⁴⁺Mn₃³⁺(μ_3 -O²⁻)₃(μ_3 -F⁻)(OAc)₃(dbm)₃⁻ (**1**) molecule [5,6].

The molecule (**1**) contains three dbm groups. Each dbm group, (CH(COC₆H₅)₂), contain two C₆H₅ rings, as depicted in Fig. 2(a). Replacing each C₆H₅ ring with an isovalent H atom, i.e., substituting CH(COC₆H₅)₂ with CH(CHO)₂ (a procedure also known as “hydrogen saturation”) the molecule (**1**) resizes to Mn⁴⁺Mn₃³⁺(μ_3 -O²⁻)₃(μ_3 -F⁻)(OAc)₃(CH(CHO)₂)₃⁻ (**2**) molecule, see panel (b) of Fig. 2. A comparison between (**1**) and (**2**) show that their Mn₄L₃F(OAc)₃ skeletons are nearly the same. For example, the difference in α and d_{AB} of these molecules are very small, as shown in Table 1. Also their magnetic moments at Mn sites and J_{AB} are nearly the same. It is noted that the molecule (**1**) is obtained from the molecule (**2**) by replacing each C₆H₅ ring of dbm groups with one H atom. These results demonstrate that variation in outer part of dbm groups is not so much influence on magnetic properties of Mn₄ molecules. This finding is very helpful, since the computational cost can be significantly reduced. Next, new distorted cubane Mn⁴⁺Mn₃³⁺ will be designed based on the molecule (**2**).

In the molecule (**2**), the μ_3 -O atoms form Mn⁴⁺-(μ_3 -O)-Mn³⁺ exchange pathways between the Mn⁴⁺ and Mn³⁺ ions, as shown in Fig. 3. Therefore, substituting μ_3 -O with other ligands will be an effective way to tailor the geometric structure of exchange pathways between the Mn⁴⁺ and Mn³⁺ ions, as well as the exchange coupling between

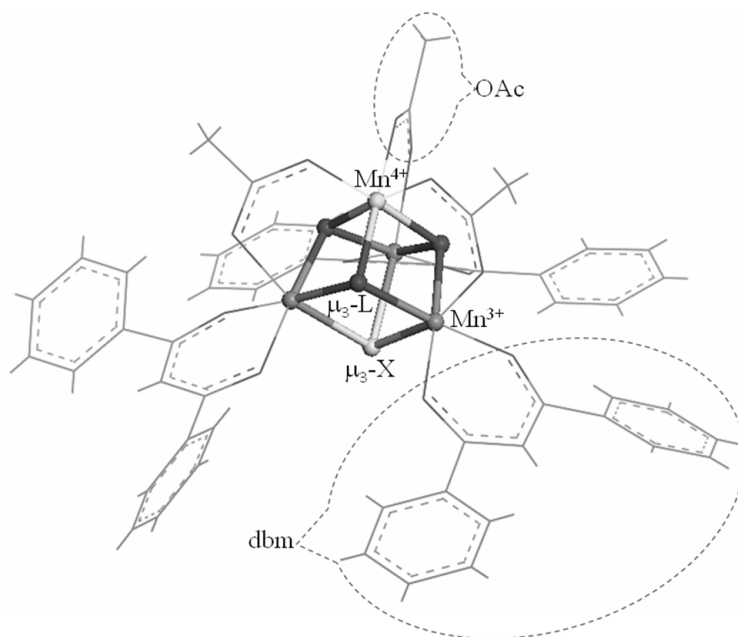


Fig. 1. The schematic geometric structure of $[\text{Mn}^{4+}\text{Mn}_3^{3+}(\mu_3\text{-L}^{2-})_3(\mu_3\text{-X}^-)(\text{OAc})_3^-(\text{dbm})_3^-]$ molecules (the atoms in the distorted cubane $[\text{Mn}^{4+}\text{Mn}_3^{3+}(\mu_3\text{-L}^{2-})_3(\mu_3\text{-X}^-)]$ core are highlighted in the ball).

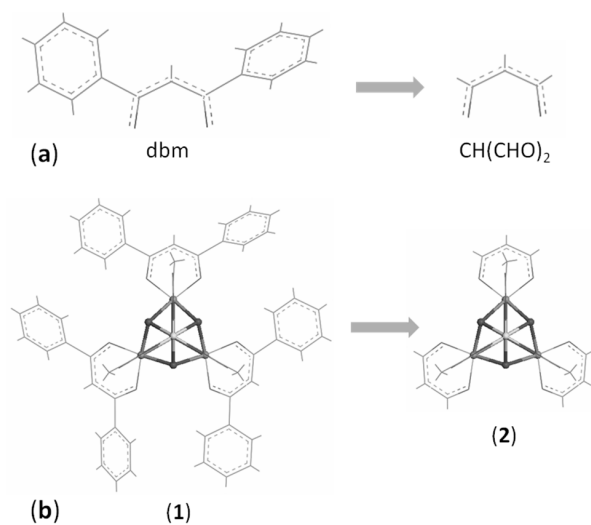


Fig. 2. Schematic presentation of the pruning procedure adopted for molecule (1).

them. To preserve the distorted cubane geometry of the core of $\text{Mn}^{4+}\text{Mn}_3^{3+}$ molecules and the formal charges of Mn ions, ligands substituted for the core $\mu_3\text{-O}$ ligand should

Table 1. This table shows stability of geometric structure and magnetic properties of Mn⁴⁺Mn₃³⁺ molecules by substituting dbm with CH(CHO)₂: some selected bond lengths (Å) and bond angles (deg) of the [Mn⁴⁺Mn₃³⁺(μ₃-O²⁻)₃(μ₃-F⁻)] core, the magnetic moments (in μ_B unit) at Mn⁴⁺(*m*_A) and Mn³⁺(*m*_B) ions, and the *J*_{AB}/*k*_B (in K unit). The relative changes (%) of these quantities are very small.

	Mn ⁴⁺ -(μ ₃ -O)-Mn ³⁺	Mn ⁴⁺ -Mn ³⁺	Mn ⁴⁺ -(μ ₃ -O)	Mn ³⁺ -(μ ₃ -O)	<i>m</i> _A	<i>m</i> _B	<i>J</i> _{AB} / <i>k</i> _B
(1)	95.037	2.834	1.907	1.947	-2.703	3.896	-73.51
(2)	95.060	2.840	1.907	1.944	-2.692	3.907	-75.15
%	0.02	0.21	0.00	0.15	0.41	0.28	2.23

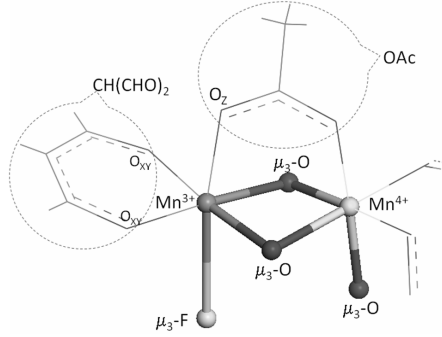


Fig. 3. Schematic presentation of ligand configuration at the Mn³⁺ and Mn⁴⁺ sites of the molecule (2).

satisfy following conditions: (i) To have the valence of 2; (ii) The ionic radius of these ligands should be not so different from that of O²⁻ ion. From these remarks, N based ligands, NR (R = a radical), should be the best candidates. Moreover, by variation in R group, the local electronic structure as well as electronegativity at N site can be controlled. As a consequence, the Mn-N bond lengths and the Mn⁴⁺-N-Mn³⁺ angles (α), as well as delocalization of *d*₂₂ electrons from the Mn³⁺ sites to the Mn⁴⁺ site and *J*_{AB} are expected to be tailored. By variations in μ₃-O ligands, new seven Mn⁴⁺Mn₃³⁺ molecules have been designed. These molecules have a general chemical formula [Mn⁴⁺Mn₃³⁺(μ₃-L²⁻)₃(μ₃-F⁻)(OAc)₃⁻(CH(CHO)₂)₃⁻] with L = NSiH₃, NCSiH₃, NSi₂H₃, NSiCH₃, NCSiH₅, NSi₂H₅, or NSiCH₅. These seven Mn⁴⁺Mn₃³⁺ molecules are labeled from (3) to (9), and their chemical formulas are tabulated in Table 2.

III.2. The geometric and electronic structures

Our calculated results show that the most magnetic stable state of all seven Mn⁴⁺Mn₃³⁺ molecules is the AFM-HS. It means that the three Mn³⁺ ions at the B sites exist in the HS state with configuration *d*⁴(*t*_{2g}³, *e*_g¹), and the exchange coupling between the three Mn³⁺ ions and the Mn⁴⁺ ion is AFM resulting in the ferrimagnetic structure in Mn⁴⁺Mn₃³⁺ molecules with the large *S*_T of 9/2. Note that, the HS state with configuration *d*⁴(*t*_{2g}³, *e*_g¹) relates to the appearance of the elongated Jahn-Teller distortions at Mn³⁺ ions.

Table 2. The chemical formulas of molecules (3)–(9), and their L ligands. Selected important magnetic and geometric parameters of molecules (3)–(9), the magnetic moment at Mn sites (m_A and m_B in μ_B), the effective exchange coupling parameter between the Mn^{4+} and Mn^{3+} ions (J_{AB}/k_B in K), the exchange coupling angle $\text{Mn}^{4+}-\mu_3-\text{O}^{2-}-\text{Mn}^{3+}$ (α in degree), the distance between the Mn^{4+} and Mn^{3+} ions (d_{AB} in Å), and the distortion factor of B sites (f_{dist} in %).

	L	$\text{Mn}^{4+}\text{Mn}_3^{3+}$ molecules	m_A	m_B	J_{AB}/k_B	α	d_{AB}	f_{dist}
(3)	NSiH ₃	$\text{Mn}_4(\text{NSiH}_3)_3\text{F}(\text{OAc})_3(\text{CH}(\text{CHO})_2)_3$	-2.642	3.918	-137.10	91.188	2.833	11.750
(4)	NCSiH ₃	$\text{Mn}_4(\text{CSiH}_3)_3\text{F}(\text{OAc})_3(\text{CH}(\text{CHO})_2)_3$	-2.447	4.084	-110.31	90.353	2.850	8.632
(5)	NSi ₂ H ₃	$\text{Mn}_4(\text{NSi}_2\text{H}_3)_3\text{F}(\text{OAc})_3(\text{CH}(\text{CHO})_2)_3$	-2.620	4.017	-107.05	91.534	2.873	13.260
(6)	NSiCH ₃	$\text{Mn}_4(\text{NSiCH}_3)_3\text{F}(\text{OAc})_3(\text{CH}(\text{CHO})_2)_3$	-2.624	3.988	-107.22	91.650	2.871	13.670
(7)	NCSiH ₅	$\text{Mn}_4(\text{NCSiH}_5)_3\text{F}(\text{OAc})_3(\text{CH}(\text{CHO})_2)_3$	-2.501	3.888	-196.53	89.192	2.779	10.944
(8)	NSi ₂ H ₅	$\text{Mn}_4(\text{NSi}_2\text{H}_5)_3\text{F}(\text{OAc})_3(\text{CH}(\text{CHO})_2)_3$	-2.624	3.906	-149.92	90.388	2.818	11.069
(9)	NSiCH ₅	$\text{Mn}_4(\text{NSiCH}_5)_3\text{F}(\text{OAc})_3(\text{CH}(\text{CHO})_2)_3$	-2.625	3.911	-151.55	90.280	2.814	11.360

Our calculated results confirm that each of three Mn^{3+} sites is an elongated octahedron along the Mn^{3+}O_Z axis. Here, the distortion factor of the B sites is measured by $f_{dist} = \frac{d_Z - d_{XY}}{d_{XY}} \times 100\%$, where, d_Z is the interatomic distance between the Mn^{3+} and O_Z sites as labeled in Fig. 3. The d_{XY} is the average interatomic distance between the Mn^{3+} site and the two O sites of the $\text{CH}(\text{CHO})_2$ group as shown in Fig. 3. The value of f_{dist} is tabulated in Table 2, in which molecule (6) with L = NSiCH₃ has the highest value of $f_{dist} = 13.670\%$, the molecule (4) with L = NCSiH₃ has the smallest value of $f_{dist} = 8.632\%$. The HS spin state as well as the elongated Jahn-Teller distortions at Mn^{3+} ions is known as one of the origin of the axial anisotropy in Mn SMMs [15–17]. These results demonstrate that all seven $\text{Mn}^{4+}\text{Mn}_3^{3+}$ molecules must have axial anisotropy. Therefore, they are high-spin anisotropic molecules. Next, we will present in detail about the geometric structure and magnetic properties of these seven $\text{Mn}^{4+}\text{Mn}_3^{3+}$ molecules. The geometric structures corresponding to the most stable states of these seven $\text{Mn}^{4+}\text{Mn}_3^{3+}$ molecules are depicted in Fig. 4.

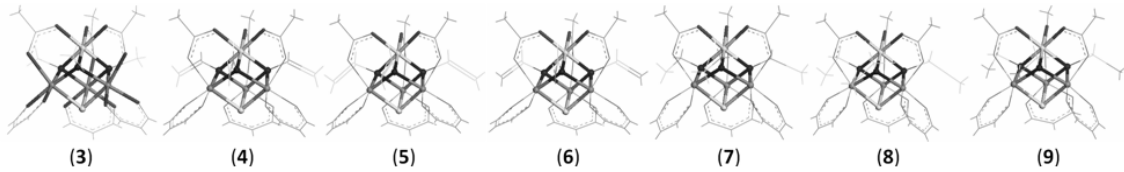


Fig. 4. The schematic geometric structure of molecules (3)–(9).

Our calculations confirm that the C_{3v} symmetry of $\text{Mn}^{4+}\text{Mn}_3^{3+}$ molecules, with the C_{3v} axis passing through the Mn^{4+} and $\mu_3\text{-F}^-$ sites, is preserved even if the L ligands are changed. Also the distorted cubane geometry of the $\text{Mn}^{4+}\text{Mn}_3^{3+}$ core is preserved. However, their bond angles and interatomic distances are various, in which the exchange coupling angle (α) and the $\text{Mn}^{3+}\text{-Mn}^{4+}$ interatomic distance (d_{AB}) are changed in the ranges of $89.192^\circ\text{--}91.650^\circ$ and $2.779\text{\AA}\text{--}2.873\text{\AA}$, respectively, as tabulated in Table 2. As

expected, the exchange coupling parameter J_{AB} is also various, as shown in Table 2. These seven Mn⁴⁺Mn₃³⁺ molecules have the J_{AB} are from 1.5 to 3 times stronger than that of the molecule (1), and their α is around 90°. It is noted that the molecule (1) has the α of 95.037°. The calculated results confirm the expectation that J_{AB} tends to become stronger when the α reaches to around 90°. The molecule (7) with L = NCSiH₅ has the highest J_{AB}/k_B of -196.53 K corresponding to $\alpha = 89.192^\circ$. This value is about 3 times larger than that of (1). These results demonstrate the advantages of employing N-based ligands (NR, R = various) instead of oxygen to form exchange pathways between Mn atoms in distorted cubane Mn₄ molecules. Variation in R group is an effective way to tailor exchange couplings between Mn atoms.

Also, as shown in Fig. 5, the J_{AB} tends to become stronger with decrease of d_{AB} which can be attributed to increase of direct overlap between 3d orbitals at the A and B sites.

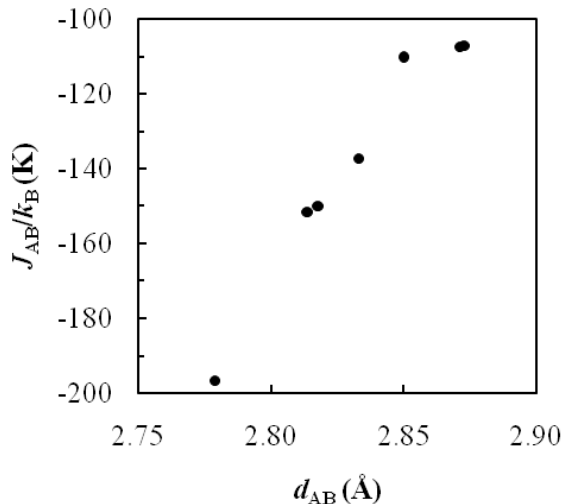


Fig. 5. The d_{AB} dependence of J_{AB} of molecules (3)-(9).

IV. CONCLUSION

By employing N-based ligands to form the exchange pathways between Mn atoms, new seven high-spin anisotropic molecules $[\text{Mn}^{4+}\text{Mn}_3^{3+}(\mu_3\text{-L}^{2-})_3(\mu_3\text{-F}^-)_3(\text{CH}(\text{CHO})_2)_3]^-$ (L = NSiH₃, NCSiH₃, NSi₂H₃, NSiCH₃, NCSiH₅, NSi₂H₅, or NSiCH₅) with S_T of 9/2 have been designed. These seven molecules (3)-(9) have the J_{AB} being from 1.5 to 3 times stronger than that of the molecule (1), and their α is around 90°. The calculated results demonstrate that J_{AB} tends to become stronger when α reaches to around 90°. The molecule (7) with L = NCSiH₅ has the highest J_{AB}/k_B of -196.53 K corresponding to $\alpha = 89.192^\circ$. This value is about 3 times larger than that of synthesized Mn⁴⁺Mn₃³⁺ SMMs. These results demonstrate the advantages of employing N-based ligands (NR) instead of oxygen to form exchange pathways between Mn atoms in distorted cubane Mn₄ molecules. Variation in R group is an effective way to tailor exchange couplings between Mn atoms. The results would give some hints for synthesizing new SMMs.

ACKNOWLEDGMENTS

We thank the Vietnam's National Foundation for Science and Technology Development (NAFOSTED) for funding this work within project 103.01.77.09. The computations presented in this study were performed at the Information Science Center of Japan Advanced Institute of Science and Technology, and the Center for Computational Science of the Faculty of Physics, Hanoi University of Science, Vietnam.

REFERENCES

- [1] L. Bogani and W. Wernsdorfer, *Nature Materials*. **7** (2008) 179.
- [2] A. Saitoh, H. Miyasaka, M. Yamashita and R. Clérac, *J. Mater. Chem.* **17** (2007) 2002.
- [3] B. J. Milios, A. Vinslava, W. Wernsdorfer, S. Moggach, S. Parsons, S. P. Perlepes, G. Christou, and E. K. Brechin, *J. Am. Chem. Soc.*, **129** (2007) 2754.
- [4] V. Marvaud, J. M. Herrera, T. Barilero, F. Tuyeras, R. Garde, A. Sculler, C. Decroix, M. Cantuel, and C. Desplanches, *Monatshefte für Chemie*. **134** (2003) 149.
- [5] H. Andres, R. Basler, H. Güdel, G. Aromí, G. Christou, H. Büttner, and B. Rufflé. *J. Am. Chem. Soc.* **122** (2000) 12469.
- [6] M. W. Wemple, D. M. Adarm, K. Folting, D. N. Hendrickson, and G. Christou, *J. Am. Chem. Soc.* **117** (1995) 7275.
- [7] N. A. Tuan, S. Katayama, D. H. Chi, *Phys. Chem. Chem. Phys.* **11** (2009) 717.
- [8] N. A. Tuan, S. Katayama, D. H. Chi, *Comput. Mater. Sci.* **44** (2008) 111.
- [9] M. J. Han, T. Ozaki, and J. Yu, *Phys. Rev. B* **70** (2004) 184421.
- [10] K. Park, M. R. Pederson, and N. Bernstein, *J. Phys. Chem. Solids*. **65** (2004) 805.
- [11] B. Delley, *J. Chem. Phys.* **92** (1990) 508.
- [12] B. Hammer, L. B. Hansen, J. K. Nørskov, *Phys. Rev. B* **59** (1999) 7413.
- [13] B. Delley. *Int. J. Quant. Chem.* **69** (1998) 423.
- [14] R. S. Mulliken, *J. Chem. Phys.* **23** (1955) 1833; R. S. Mulliken, *J. Chem. Phys.* **23** (1955) 1841.
- [15] R. Sessoli, H.-L. Tsai, A. R. Schake, S. Wang, J. B. Vincent, K. Folting, D. Gatteschi, G. Christou, and D. N. Hendrickson, *J. Am. Chem. Soc.* **115** (1993) 1804.
- [16] C.-I. Yang, W. Wernsdorfer, G. -H, Lee, and H.-L. Tsai, *J. Am. Chem. Soc.* **129** (2007) 456 .
- [17] H. Miyasaka, T. Madanbashi, K. Sugimoto, Y. Nakazawa, W. Wernsdorfer, K. Sugiura, M. Yamashita, C. Coulon, and R. Clérac, *Chem. Eur. J.* **12** (2006) 7028.

Received 10 October 2010.